Challenge Journal of Structural Mechanics

Research Article

Evaluation of artificial neural network-based formulations for tuned mass dampers

Melda Yucel [a,*], Sinan Melih Nigdeli [a], Gebrail Bekdaş [a]

[a] *Department of Civil Enginering, İstanbul University-Cerrahpaşa, 34320 İstanbul, Turkey*

ABSTRACT

Tuned mass dampers (TMDs) are used to damp vibration of mechanical systems. TMDs are also used on structures to reduce the effects of strong forces such as winds and earthquakes. For the efficiency of TMD, optimization of TMD parameters is needed. Several classical formulations were proposed, but metaheuristic methods are generally used to find the best result. In addition, the metaheuristic based optimum results are used in machine learning of artificial intelligence-based models like artificial neural networks (ANN). These ANN models are also used in development of tuning equation via curve fitting. The classical and ANN-based formulations were found according to frequency domain responses. In the present study, the classical and ANN-based formulations were evaluated by comparing on time-history responses of seismic structure. In comparison, near-fault ground motion records including directivity pulses are used. The ANN based methods have advantages by providing smaller stroke requirement and damping for TMDs.

ARTICLE INFO

Article history:
Received 29 August 2020
Revised 13 October 2020
Accepted 23 October 2020

Keywords:
Artificial neural networks
Tuned mass dampers
Structural control
Optimization
near-fault
Metaheuristic

1. Introduction

In order to reduce structural vibrations, several control methods have been proposed. These methods may be passive, active, semi-active or hybrid control methods. All systems of different control strategies need to be optimized to find a perfect tuning of parameters according to controlled structure subjected to vibration sources like earthquakes, winds and traffics.

Tuned mass dampers are passive vibration control devices which are used in general mechanical systems. For this purpose, several simplified equations are proposed (Den Hartog, 1947; Warburton, 1982; Sadek et al., 1997; Leung and Zhang, 2009; Yucel et al., 2019). These equations were derived according to mathematical equations, curve fitting of numerical iteration and optimum results as details given in Section 2.1.

In recent years, the most chosen methods for optimum tuning of mass dampers is the usage of metaheuristic methods. As examples, the usage of harmony search (HS) (Bekdaş and Nigdeli, 2011; Nigdeli and Bekdaş, 2017), particle swarm optimization (Khatibinia et al., 2016), ant colony algorithm (Viana et al., 2008), genetic algorithm (Mohebbi et al., 2013; Pourzeynali et al., 2013; Arfiadi, 2016), artificial bee colony optimization (Farshidianfar and Soheili, 2013), simulated annealing (Yang and Li, 2016), cuckoo search (Etedali and Mollayi, 2018), gravitational algorithm (Khatibinia et al., 2018), bat algorithm (Bekdaş et al., 2018) and flower pollination (FPA) (Bekdaş et al., 2017); besides the usage of both harmony search, flower pollination algorithm, teaching-learning based optimization and jaya algorithm (Bekdaş et al., 2019) were proposed to optimize different types of TMDs for different objectives about responses of structures.

The process of numerical optimization method may need high amount of computation time. For that reason, Yucel et al. (2019) used the optimum TMD parameters on machine learning of an artificial neural network (ANN) model, and several equations were developed for easy use of engineers.

The classical and ANN-based formulations were found according to frequency-domain response of structures. The exact effect of TMDs can be only seen on time-history responses. For that reason, several formulations

* *Corresponding author.* E-mail address: melda.yucel@yahoo.com.tr (M. Yucel)
ISSN: 2149-8024 / DOI: https://doi.org/10.20528/cjsmec.2021.01.003

are investigated on time-history responses of seismic structures by using near-fault ground motions. As seen in Fig. 1, near fault ground motion have two significant impulsive motions.

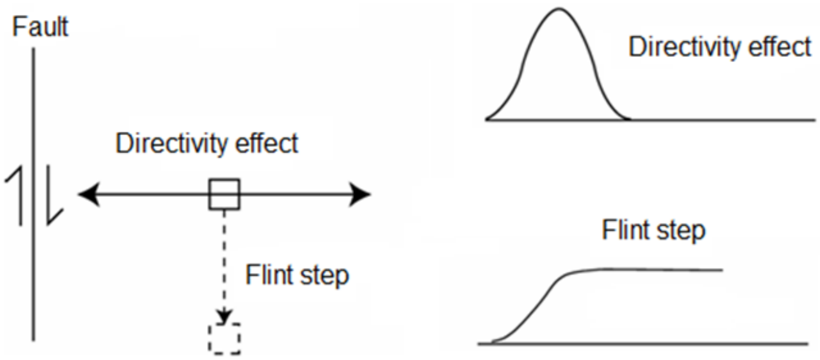

Fig. 1. Impulsive motions.

Directivity pulses, which are critically effective on structures, occur in the direction perpendicular to fault (Steward et al., 2001). These pulses have long period and high peak ground velocity. In FEMA P-695: Quantification of Building Seismic Performance Factors (2009), several near fault ground motion records with pulses are grouped, and these records given in Table 1 were used in the present study.

Table 1. Earthquake set for near-field excitations with pulses (FEMA P-695, 2009).

Earthquake No.	Earthquake Name	Recording Station	Year	Magnitude
1	Imperial Valley-06	El Centro Array #6	1979	6.5
2	Imperial Valley-06	El Centro Array #7	1979	6.5
3	Irpinia, Italy-01	Sturno	1980	6.9
4	Superstition Hills-02	Parachute Test Site	1987	6.5
5	Loma Prieta	Saratoga – Aloha	1989	6.9
6	Erzican, Turkey	Erzican	1992	6.7
7	Cape Mendocino	Petrolia	1992	7.0
8	Landers	Lucerne	1992	7.3
9	Northridge-01	01 Rinaldi Receiving Sta	1994	6.7
10	Northridge-01	01 Sylmar - Olive View	1994	6.7
11	Kocaeli, Turkey	Izmit	1999	7.5
12	Chi-Chi, Taiwan	TCU065	1999	7.6
13	Chi-Chi, Taiwan	TCU102	1999	7.6
14	Duzce, Turkey	Duzce	1999	7.1

2. Design of Tuned Mass Dampers

2.1. Equations of motion

In Fig. 2, a TMD attached to a single degree of freedom (SDOF) structures is shown. $\ddot{x}_g$ is the recorded acceleration of ground motions. The response of the structure is the displacement (x). The structural parameters taken as the design constants are the mass (m), stiffness (k) and the damping coefficient (c), which are found according to the inherent damping (ξ) of the structure as given in Eq. (1).

$$c = 2m\xi\sqrt{\frac{k}{m}} \tag{1}$$

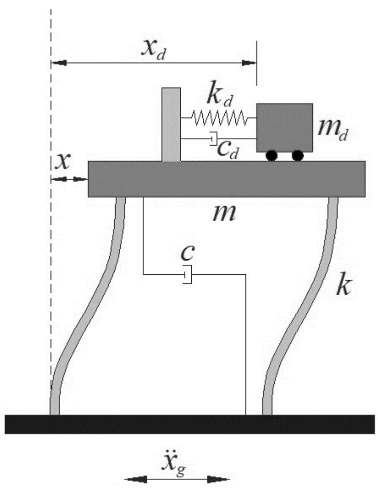

Fig. 2. SDOF structure with TMD.

The parameters of TMD are mass (m_d), stiffness (k_d) and damping coefficient (c_d) of the structure. Generally, the mass of TMD is optimum at the highest allowed value according to axial loading capacity of the structure. In tuning formulations, mass ratio (μ) is defined as given in Eq. (2).

$$\mu = \frac{m_d}{m} \tag{2}$$

In matrix form, the equation of motion of structure coupled with a TMD is given as Eq. (3). The mass, damping and stiffness matrices are shown as M, C and K, respectively. These matrices and the displacement vector ($x(t)$) are shown in Eqs. (4-7).

$$M\ddot{x}(t) + C\dot{x}(t) + Kx(t) = -M[1]\ddot{x}_g(t) \tag{3}$$

$$M = \begin{bmatrix} m & 0 \\ 0 & m_d \end{bmatrix} \tag{4}$$

$$C = \begin{bmatrix} c + c_d & -c_d \\ -c_d & c_d \end{bmatrix} \tag{5}$$

$$K = \begin{bmatrix} k + k_d & -k_d \\ -k_d & k_d \end{bmatrix} \tag{6}$$

$$x(t) = \begin{Bmatrix} x \\ x_d \end{Bmatrix} \tag{7}$$

The dots on $x(t)$ represent a derivative of $x(t)$ respect to time. Solving of x needs long calculation time, and the results are specific for the excited ground acceleration. Due to that, the response can be investigated in frequency domain (ω) by calculating the amplitude (f) of transfer function (TF(ω)). TF(ω) is the ratio of Laplace transformations of acceleration of the system and ground. TF(ω) and f are formulated as Eqs. (8) and (9), respectively.

$$TF(\omega) = \begin{bmatrix} TF \\ TF_d \end{bmatrix} = [-M\omega^2 + C\omega j + K]^{-1} M\omega^2\{1\} \tag{8}$$

$$f = 20\text{Log}_{10}|\max(TF)| \tag{9}$$

2.2. Tuning equations for TMDs

In Table 2, the compared tuning equations with ANN-based equations are given. The equations are for optimum frequency ratio (f_{opt}) and optimum damping ratio TMD ($\xi_{d,\text{opt}}$). f_{opt} and $\xi_{d,\text{opt}}$ are formulated as Eqs. (10) and (11), respectively.

Table 2. The frequency and damping ratio expressions of the compared methods.

Method	f_{opt}	$\xi_{d,\text{opt}}$
Den Hartog (1947)	$\frac{1}{1+\mu}$	$\sqrt{\frac{3\mu}{8(1+\mu)}}$
Warburton (1982)	$\frac{\sqrt{1-\left(\frac{\mu}{2}\right)}}{1+\mu}$	$\sqrt{\frac{\mu\left(1-\frac{\mu}{4}\right)}{4(1+\mu)\left(1-\frac{\mu}{2}\right)}}$
Sadek et al. (1997)	$\frac{1}{1+\mu}\left[1-\xi\sqrt{\frac{\mu}{1+\mu}}\right]$	$\frac{\xi}{1+\mu}+\sqrt{\frac{\mu}{1+\mu}}$
Leung and Zhang (2009)	$\frac{\sqrt{1-\left(\frac{\mu}{2}\right)}}{1+\mu} + (-4.9453 + 20.2319\sqrt{\mu} - 37.9419\mu)\sqrt{\mu}\xi + (-4.8287 + 25.0000\sqrt{\mu})\sqrt{\mu}\xi^2$	$\sqrt{\frac{\mu\left(1-\frac{\mu}{4}\right)}{4(1+\mu)\left(1-\frac{\mu}{2}\right)}} - 5.3024\xi^2\mu$

$$f_{opt} = \frac{\omega_d}{\omega_s} \tag{10}$$

$$\xi_{d,\text{opt}} = \frac{c_d}{2m_d\omega_d} \tag{11}$$

$\omega_{d,\text{opt}}$ is the frequency of the TMD as given in Eq. (12), and ω_s is the frequency of single degree of freedom (SDOF) structure as shown in Eq. (13).

$$\omega_d = \sqrt{\frac{k_d}{m_d}} \tag{12}$$

$$\omega_s = \sqrt{\frac{k}{m}} \tag{13}$$

The equation of Den Hartog (1947) was found for harmonic excitations. Warburton (1982) derived the formulation for white-noise excitation. Sadek et al. (1997) used curve-fitting of numerical optimization results to find a formulation including the effect of inherent damping of the structure. Leung and Zhang (2009) employed PSO to find the TMD tuning equations.

2.3. ANN-based formulation for TMD optimization

Artificial neural networks (ANN) are an artificial intelligence modelling tool, and it based on simulating human brain behavior on different systems. Via ANN, it is possible estimate final results without processing the solving of problems. Yucel et al. (2019) developed an ANN model for optimization of TMDs providing optimum period (T_d) and damping ratio ($\xi_{d,\mathrm{opt}}$) of TMDs. The relationship between T_d and stiffness of TMD (k_d) is given as Eq. (14).

$$T_d = 2\pi\sqrt{\frac{m_d}{k_d}} \tag{14}$$

The structure of the developed ANN model is shown as Fig. 3. The inputs are the period (T_s) of SDOF structure given as Eq. (15) and mass ratio (μ).

$$T_s = 2\pi\sqrt{\frac{m}{k}} \tag{15}$$

In machine learning of the ANN model, FPA algorithm developed by Yang (2012) was used. The methodology given in Bekdaş et al. (2017) was used to find the optimum TMD values for different cases of SDOF structures. The developed ANN model was used to find the simplified equations given in Table 3.

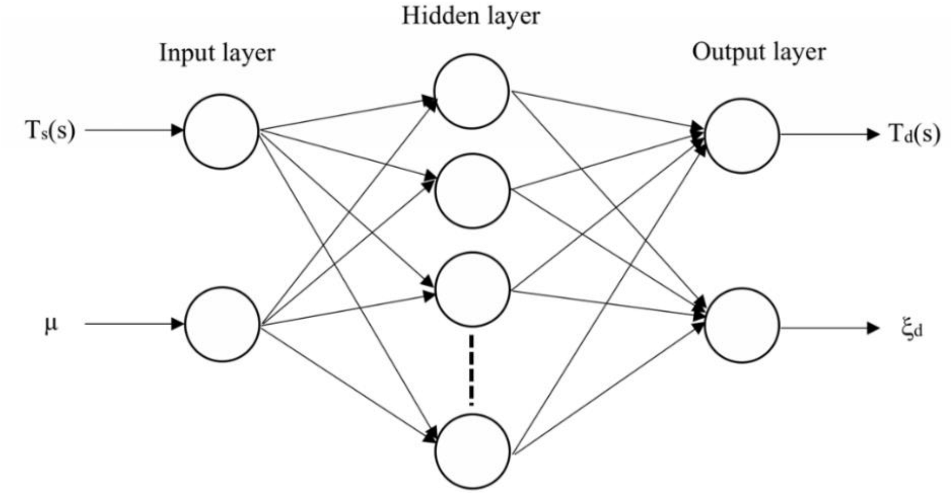

Fig. 3. ANN structure.

Table 3. ANN based formulations (Yucel et al., 2019).

Method	f_{opt}	$\xi_{d,\mathrm{opt}}$
Linear	$f_{\mathrm{opt}} = -0.6438\mu + 0.9966$	$\xi_{d,\mathrm{opt}} = -0.5673\mu + 0.1235$
Polynomial	$f_{\mathrm{opt}} = -249.91\mu^5 + 400.09\mu^4$ $-208.03\mu^3 + 43.801\mu^2 - 4.1453\mu + 1.0675$	$\xi_{d,\mathrm{opt}} = -54.673\mu^4 + 54.639\mu^3 - 19.274\mu^2$ $+3.2302\mu + 0.0237$
Exponential	$f_{\mathrm{opt}} = 1.0038\, e^{-0.747\mu}$	$\xi_{d,\mathrm{opt}} = 1.1258\, e^{2.8573\mu}$

3. Comparison of the methods

The investigations were done for four cases of SDOF structure period. All structures were also tested for three mass ratio values. The cases are shown in Tables 4 and 5.

The results of different methods are presented in Tables 6-9 including the sub-cases of mass ratio in Appendix. Also, the comparisons intended for x, a and stroke values within these results of formulations, which were proposed in literature and developed as ANN-based, can be seen in Fig. 4-7 for case 1-4, respectively. The results include the optimum TMD values, maximum displacement (x) and acceleration (a) of the structure. Also, stroke values are presented for the TMD. The presented stroke value is a normalized value as given in Eq. (16).

$$stroke = \frac{max(|x_d|) - max(|x|)}{max(|x|)_{structure\ without\ TMD}} \tag{16}$$

Table 4. Numerical cases for periods.

Case	T_s (s)
1	0.5
2	1
3	2
4	4

Table 5. Numerical cases for mass ratio.

Case	μ
a	0.05
b	0.10
c	0.20

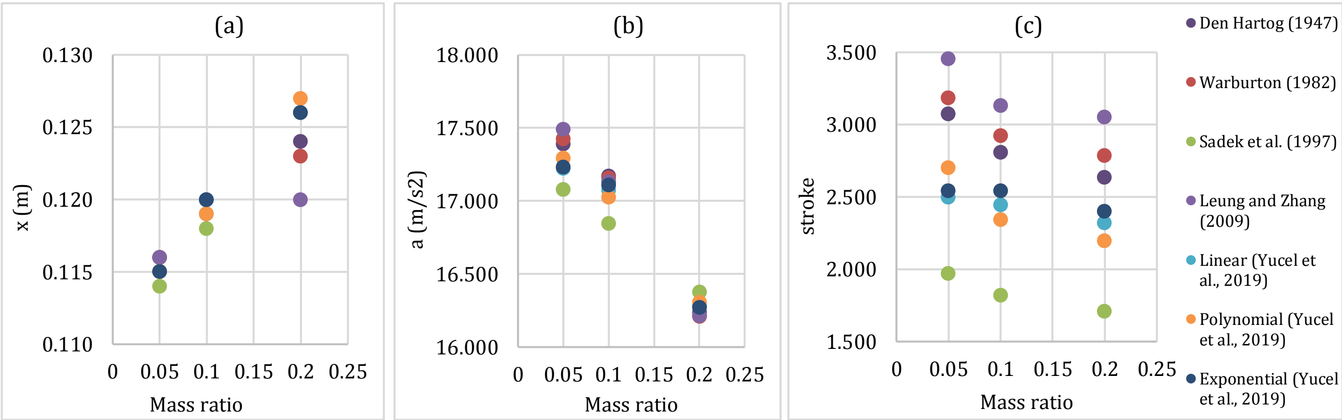

Fig. 4. The numerical results (Case 1): (a) x (m); (b) a (m/s^2); (c) stroke.

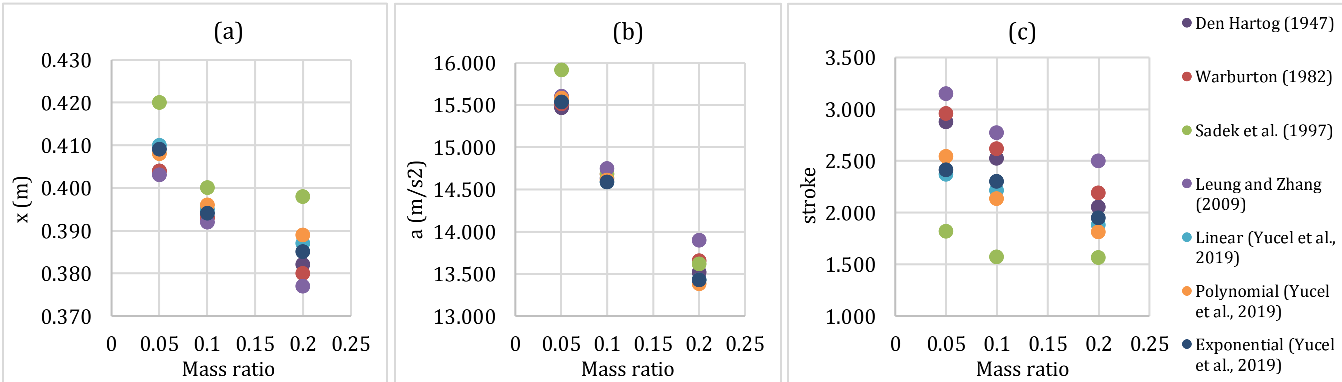

Fig. 5. The numerical results (Case 2): (a) x (m); (b) a (m/s^2); (c) stroke.

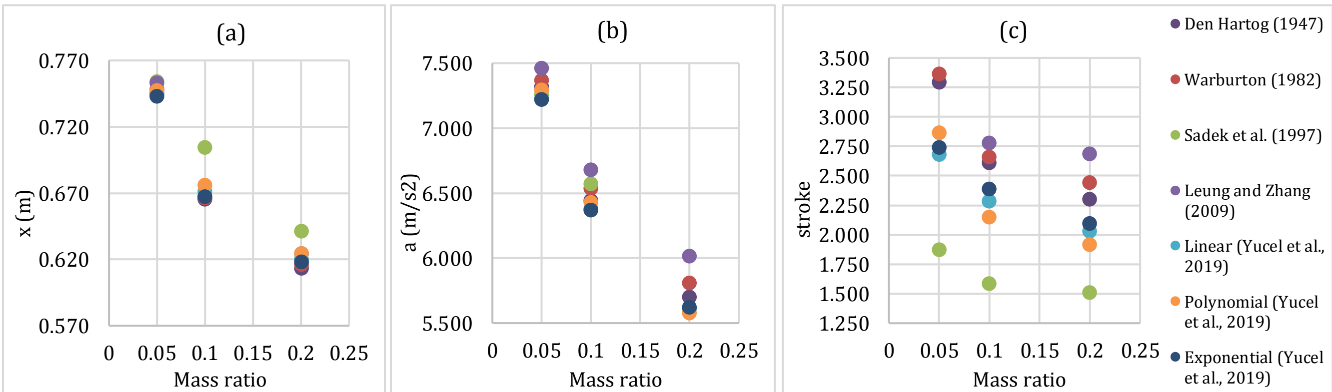

Fig. 6. The numerical results (Case 3): (a) x (m); (b) a (m/s^2); (c) stroke.

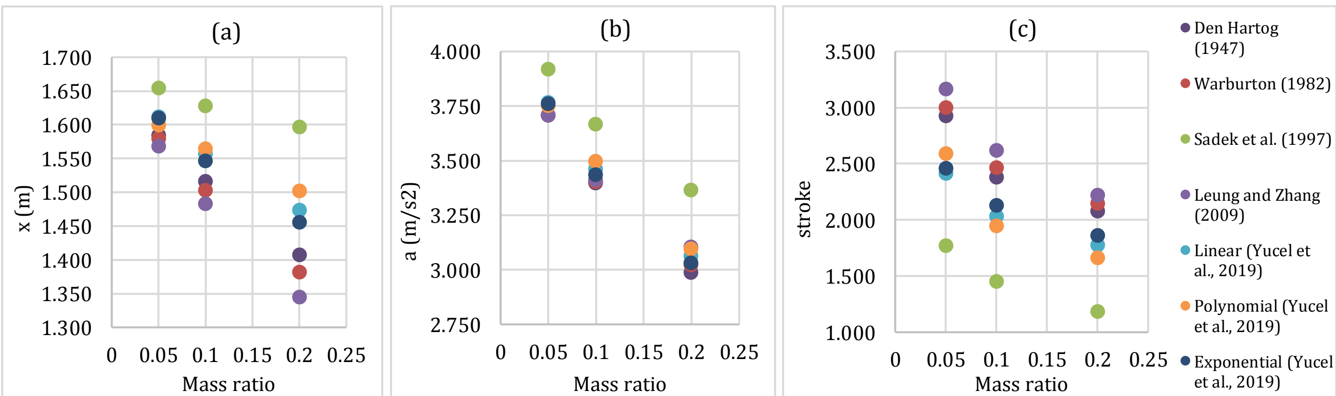

Fig. 7. The numerical results (Case 4): (a) x (m); (b) a (m/s^2); (c) stroke.

4. Conclusions

In general, the ANN-based formulations are more effective than all formulations (except of Sadek et al. (1997)). When the optimum damping ratios of TMDs are investigated, Sadek et al. (1997) have a very big optimum value comparing to ANN-based method. Thus, the optimum TMD designed according to Sadek et al. (1997) have a high cost. By the increase of the damping, control can be provided with a small stroke value. The ANN-based methods have also small stroke values comparing to the others. By the increase of mass ratio, the damping values are increasing, and the values of Sadek et al. (1997) (4.5%) may need a high cost design. The effectiveness of the ANN-based formulations can be best seen in average results of response under different excitations.

While ANN-based methods (Yucel et al., 2019) and Sadek et al. (1997) are the best in reduction of maximum responses, the classical methods like Den Hartog and Warburton may be more effective for long period structures. For the same cases of 4s period SDOF structure, the best method is PSO-based formulations (Leung and Zhang, 2009).

In total, the ANN-based method provides comparative solutions with a feasible TMD design. The success of optimum values is both seen for the displacement and the acceleration values. By the increase of the mass ratio, a small advantage of the exponential equations can be seen, while all three types have similar performances.

Appendix

Table 6. The numerical values (Case 1).

		SDOF without TMD	Den Hartog (1947)	Warburton (1982)	Sadek et al. (1997)	Leung and Zhang (2009)	Linear (Yucel et al., 2019)	Polynomial (Yucel et al., 2019)	Exponential (Yucel et al., 2019)
					μ=0.05				
	T_d (s)		0.525	0.532	0.531	0.547	0.518	0.528	0.517
	ξ_d (%)		10.911	10.981	26.584	10.914	15.187	14.351	14.512
Critical	x (m)	0.124	0.116	0.116	0.114	0.116	0.115	0.115	0.115
Critical	a (m/s^2)	19.761	17.391	17.426	17.077	17.492	17.224	17.295	17.233
Critical	stroke		3.076	3.185	1.972	3.457	2.499	2.702	2.544
Mean	x (m)	0.051	0.048	0.048	0.049	0.048	0.048	0.048	0.048
Mean	a (m/s^2)	8.119	7.280	7.284	7.314	7.308	7.268	7.272	7.267
Mean	stroke		2.380	2.428	1.540	2.543	1.999	2.124	2.033
					μ=0.10				
	T_d (s)		0.550	0.564	0.558	0.587	0.536	0.543	0.537
	ξ_d (%)		15.076	15.273	34.697	15.140	18.023	20.315	16.741
Critical	x (m)	0.124	0.120	0.120	0.118	0.119	0.120	0.119	0.120
Critical	a (m/s^2)	19.761	17.169	17.158	16.844	17.133	17.073	17.026	17.109
Critical	stroke		2.806	2.924	1.821	3.130	2.446	2.345	2.542
Mean	x (m)	0.051	0.048	0.048	0.049	0.047	0.049	0.048	0.049
Mean	a (m/s^2)	8.119	6.891	6.896	7.010	6.911	6.886	6.889	6.885
Mean	stroke		2.025	2.094	1.357	2.216	1.800	1.733	1.863
					μ=0.20				
	T_d (s)		0.600	0.632	0.613	0.695	0.576	0.564	0.578
	ξ_d (%)		20.412	20.972	44.991	20.707	23.696	24.842	22.277
Critical	x (m)	0.124	0.124	0.123	0.126	0.120	0.126	0.127	0.126
Critical	a (m/s^2)	19.761	16.234	16.211	16.378	16.212	16.284	16.308	16.273
Critical	stroke		2.636	2.787	1.710	3.054	2.321	2.198	2.402
Mean	x (m)	0.051	0.049	0.047	0.050	0.046	0.050	0.050	0.049
Mean	a (m/s^2)	8.119	6.326	6.317	6.585	6.382	6.369	6.405	6.360
Mean	stroke		1.841	1.945	1.253	2.170	1.627	1.545	1.682

Table 7. The numerical values (Case 2).

		SDOF without TMD	Den Hartog (1947)	Warburton (1982)	Sadek et al. (1997)	Leung and Zhang (2009)	Linear (Yucel et al., 2019)	Polynomial (Yucel et al., 2019)	Exponential (Yucel et al., 2019)
					μ=0.05				
	T_d (s)		1.050	1.063	1.062	1.093	1.037	1.057	1.034
	ξ_d (%)		10.911	10.981	26.584	10.914	15.187	14.351	14.512
Critical	x (m)	0.454	0.404	0.404	0.420	0.403	0.410	0.408	0.409
Critical	a (m/s^2)	17.987	15.466	15.510	15.915	15.604	15.560	15.582	15.532
Critical	stroke		2.878	2.959	1.821	3.149	2.368	2.543	2.414
Mean	x (m)	0.165	0.142	0.142	0.150	0.141	0.145	0.144	0.145
Mean	a (m/s^2)	6.553	5.448	5.457	5.684	5.490	5.512	5.506	5.500
Mean	stroke		2.297	2.326	1.468	2.402	1.940	2.044	1.976
					μ=0.10				
	T_d (s)		1.100	1.129	1.117	1.174	1.073	1.086	1.073
	ξ_d (%)		15.076	15.273	34.697	15.140	18.023	20.315	16.741
Critical	x (m)	0.454	0.393	0.393	0.400	0.392	0.395	0.396	0.394
Critical	a (m/s^2)	17.987	14.630	14.675	14.687	14.744	14.590	14.614	14.589
Critical	stroke		2.524	2.618	1.573	2.770	2.217	2.132	2.299
Mean	x (m)	0.165	0.139	0.138	0.144	0.137	0.141	0.141	0.140
Mean	a (m/s^2)	6.553	5.138	5.142	5.283	5.182	5.146	5.154	5.142
Mean	stroke		1.814	1.855	1.201	1.932	1.622	1.555	1.680
					μ=0.20				
	T_d (s)		1.200	1.265	1.225	1.389	1.152	1.128	1.157
	ξ_d (%)		20.412	20.972	44.991	20.707	23.696	24.842	22.277
Critical	x (m)	0.454	0.382	0.380	0.398	0.377	0.387	0.389	0.385
Critical	a (m/s^2)	17.987	13.520	13.654	13.620	13.899	13.425	13.384	13.430
Critical	stroke		2.054	2.188	1.567	2.502	1.882	1.812	1.948
Mean	x (m)	0.165	0.136	0.134	0.142	0.133	0.138	0.139	0.138
Mean	a (m/s^2)	6.553	4.756	4.786	4.849	4.882	4.731	4.731	4.731
Mean	stroke		1.519	1.587	1.041	1.746	1.354	1.290	1.400

Table 8. The numerical values (Case 3).

		SDOF without TMD	Den Hartog (1947)	Warburton (1982)	Sadek et al. (1997)	Leung and Zhang (2009)	Linear (Yucel et al., 2019)	Polynomial (Yucel et al., 2019)	Exponential (Yucel et al., 2019)
					μ=0.05				
	T_d (s)		2.100	2.127	2.123	2.186	2.074	2.114	2.068
	ξ_d (%)		10.911	10.981	26.584	10.914	15.187	14.351	14.512
Critical	x (m)	0.830	0.745	0.748	0.754	0.753	0.744	0.747	0.743
	a (m/s^2)	8.237	7.316	7.364	7.258	7.458	7.223	7.291	7.218
	stroke		3.291	3.362	1.872	3.524	2.678	2.861	2.737
Mean	x (m)	0.382	0.344	0.344	0.356	0.343	0.348	0.347	0.348
	a (m/s^2)	3.788	3.303	3.311	3.392	3.329	3.325	3.327	3.320
	stroke		2.337	2.374	1.485	2.465	1.975	2.086	2.011
					μ=0.10				
	T_d (s)		2.200	2.257	2.234	2.349	2.145	2.173	2.147
	ξ_d (%)		15.076	15.273	34.697	15.140	18.023	20.315	16.741
Critical	x (m)	0.830	0.665	0.666	0.704	0.667	0.671	0.676	0.667
	a (m/s^2)	8.237	6.442	6.533	6.571	6.677	6.376	6.427	6.369
	stroke		2.608	2.655	1.586	2.776	2.281	2.145	2.385
Mean	x (m)	0.382	0.328	0.327	0.346	0.325	0.333	0.335	0.331
	a (m/s^2)	3.788	3.053	3.072	3.178	3.108	3.065	3.085	3.055
	stroke		1.902	1.950	1.253	2.045	1.692	1.627	1.755
					μ=0.20				
	T_d (s)		2.400	2.530	2.450	2.779	2.305	2.256	2.313
	ξ_d (%)		20.412	20.972	44.991	20.707	23.696	24.842	22.277
Critical	x (m)	0.830	0.613	0.616	0.641	0.624	0.620	0.624	0.618
	a (m/s^2)	8.237	5.700	5.808	5.611	6.016	5.609	5.574	5.621
	stroke		2.301	2.442	1.508	2.685	2.026	1.917	2.094
Mean	x (m)	0.382	0.310	0.307	0.335	0.305	0.318	0.321	0.316
	a (m/s^2)	3.788	2.751	2.798	2.877	2.893	2.741	2.742	2.735
	stroke		1.600	1.670	1.064	1.811	1.424	1.356	1.472

Table 9. The numerical values (Case 4).

		SDOF without TMD	Den Hartog (1947)	Warburton (1982)	Sadek et al. (1997)	Leung and Zhang (2009)	Linear (Yucel et al., 2019)	Polynomial (Yucel et al., 2019)	Exponential (Yucel et al., 2019)
μ=0.05									
	T_d (s)		4.200	4.254	4.246	4.372	4.148	4.228	4.137
	ξ_d (%)		10.911	10.981	26.584	10.914	15.187	14.351	14.512
Critical	x (m)	1.936	1.585	1.580	1.655	1.569	1.612	1.600	1.610
Critical	a (m/s^2)	4.797	3.707	3.707	3.918	3.707	3.768	3.753	3.760
Critical	stroke		2.928	2.999	1.770	3.165	2.415	2.589	2.461
Mean	x (m)	0.639	0.591	0.591	0.599	0.590	0.593	0.592	0.592
Mean	a (m/s^2)	1.591	1.448	1.450	1.450	1.454	1.444	1.447	1.443
Mean	stroke		2.209	2.226	1.364	2.271	1.861	1.951	1.901
μ=0.10									
	T_d (s)		4.400	4.514	4.467	4.698	4.291	4.346	4.294
	ξ_d (%)		15.076	15.273	34.697	15.140	18.023	20.315	16.741
Critical	x (m)	1.936	1.517	1.503	1.628	1.483	1.557	1.565	1.547
Critical	a (m/s^2)	4.797	3.399	3.403	3.667	3.412	3.462	3.496	3.437
Critical	stroke		2.378	2.466	1.451	2.619	2.033	1.950	2.130
Mean	x (m)	0.639	0.571	0.570	0.582	0.570	0.573	0.574	0.573
Mean	a (m/s^2)	1.591	1.372	1.378	1.367	1.388	1.364	1.365	1.365
Mean	stroke		1.710	1.732	1.080	1.781	1.535	1.461	1.593
μ=0.20									
	T_d (s)		4.800	5.060	4.900	5.558	4.609	4.513	4.627
	ξ_d (%)		20.412	20.972	44.991	20.707	23.696	24.842	22.277
Critical	x (m)	1.936	1.408	1.382	1.597	1.345	1.474	1.502	1.456
Critical	a (m/s^2)	4.797	2.989	3.023	3.366	3.104	3.065	3.097	3.033
Critical	stroke		2.077	2.148	1.185	2.218	1.775	1.662	1.863
Mean	x (m)	0.639	0.542	0.540	0.563	0.537	0.548	0.551	0.546
Mean	a (m/s^2)	1.591	1.264	1.276	1.252	1.302	1.251	1.246	1.253
Mean	stroke		1.329	1.358	0.859	1.423	1.194	1.142	1.236

Publication Note

This research has previously been presented at the 6th International Conference on Harmony Search, Soft Computing and Applications (ICHSA 2020) held in İstanbul, Turkey, on July 16-17, 2020. Extended version of the research has been submitted to Challenge Journal of Structural Mechanics and has been peer-reviewed prior to the publication.

References

Arfiadi Y (2016). Reducing response of structures by using optimum composite tuned mass dampers. *Procedia Engineering*, 161, 67–72.

Bekdaş G, Kayabekir AE, Nigdeli SM, Toklu YC (2019). Tranfer function amplitude minimization for structures with tuned mass dampers considering soil-structure interaction. *Soil Dynamics and Earthquake Engineering*, 116, 552–562.

Bekdaş G, Nigdeli SM (2011). Estimating optimum parameters of tuned mass dampers using harmony search. *Engineering Structures*, 33, 2716–2723.

Bekdaş G, Nigdeli SM, Yang XS (2017). Metaheuristic based optimization for tuned mass dampers using frequency domain responses. *International Conference on Harmony Search Algorithm,* Singapore, 271–279.

Bekdaş G, Nigdeli SM, Yang XS (2018). A novel bat algorithm based optimum tuning of mass dampers for improving the seismic safety of structures. *Engineering Structures*, 159, 89–98.

Den Hartog JP (1947). Mechanical Vibrations. 3rd ed., McGraw-Hill, New York, USA.

Etedali S, Mollayi N (2018). Cuckoo search-based least squares support vector machine models for optimum tuning of tuned mass dampers. *International Journal of Structural Stability and Dynamics*, 18(2), 1850028.

Farshidianfar A, Soheili S (2013). ABC optimization of TMD parameters for tall buildings with soil structure interaction. *Interaction and Multiscale Mechanics*, 6(4), 339–356.

FEMA P-695 (2009). Quantification of Building Seismic Performance Factors. Federal Emergency Management Agency, Washington DC, USA.

Khatibinia M, Gholami H, Kamgar R (2018). Optimal design of tuned mass dampers subjected to continuous stationary critical excitation. *International Journal of Dynamics and Control*, 6(3), 1094–1104.

Khatibinia M, Gholami H, Labbafi SF (2016). Multi–objective optimization of tuned mass dampers considering soil–structure interaction. *Iran University of Science & Technology*, 6(4), 595–610.

Leung AYT, Zhang H (2008). Particle swarm optimization of tuned mass dampers. *Engineering Structures*, 31(3), 715–728.

Mohebbi M, Shakeri K, Ghanbarpour Y, Majzoub H (2013). Designing optimal multiple tuned mass dampers using genetic algorithms (GAs) for mitigating the seismic response of structures. *Journal of Vibration and Control*, 19(4), 605–625.

Nigdeli SM, Bekdaş G (2017). Optimum tuned mass damper design in frequency domain for structures. *KSCE Journal of Civil Engineering*, 21(3), 912–922.

Pourzeynali S, Salimi S, Kalesar HE (2013). Robust multi-objective optimization design of TMD control device to reduce tall building responses against earthquake excitations using genetic algorithms. *Scientia Iranica*, 20 (2), 207–221.

Sadek F, Mohraz B, Taylor AW, Chung RM (1997). A method of estimating the parameters of tuned mass dampers for seismic applications. *Earthquake Engineering and Structural Dynamics*, 26, 617–635.

Steward JP, Chiou S, Bray JD, Graves RW, Somerville PG, Abrahamson NA (2001). Ground Motion Evalution Procedures for Performance-Based Design. Pacific Earthquake Engineering Research Center. Report 2001/09; September 2001.

Viana FAC, Kotinda GI, Rade DA, Steffen JV (2008). Tuning dynamic vibration absorbers by using ant colony optimization. *Computers & Structures*, 86(13-14), 1539–1549.

Warburton GB (1982). Optimum absorber parameters for various combinations of response and excitation parameters. *Earthquake Engineering and Structural Dynamics*, 10, 381–401.

Yang XS (2012). Flower pollination algorithm for global optimization. *Unconventional Computation and Natural Computation,* 240–249.

Yang Y, Li C (2016). Performance of tuned tandem mass dampers for structures under the ground acceleration. *Structural Control and Health Monitoring*, 24(10), e1974.

Yucel M, Bekdaş G, Nigdeli SM, Sevgen S (2019). Estimation of optimum tuned mass damper parameters via machine learning. *Journal of Building Engineering*, 26, 100847.